SUBSECTION 2.4.4 TABLE OF CONTENTS

SUBSECTION 2.4.4 LIST OF FIGURES

2.4.4 Potential Dam Failures

The procedures described in References 2.4.4-1 and 2.4.4-2 were followed when evaluating potential flood levels from PMF and seismically induced dam failures.

The Clinch River Nuclear Site and upstream reservoirs are located in the Southern Appalachian Tectonic Province and, therefore, subject to earthquake forces with possible attendant failure of dams upstream of the CRN Site (Reference 2.4.4-3). Upstream dams whose failure has the potential to cause problems at the plant were investigated to determine if failure from seismic events would endanger plant safety. During PMF events or postulated upstream seismic failures, overtopped earthen embankments or overtopped concrete components that lacked analysis to show stability when overtopped were postulated to fail. The events analyzed are summarized in Table 2.4.3-1.

2.4.4.1 Dam and Reservoir Description

(SRI/CEII) The location of TVA projects and reservoirs with respect to the CRN Site is shown in Figure 2.4.1-5. In addition to [redacted] and [redacted] Dams upstream of the CRN Site, there are eleven projects upstream of the Watts Bar project in the Tennessee River system which influence flood levels at the CRN Site. These are [redacted] on the Little Tennessee River. Elevation-storage relationships in the major projects are shown in the twelve sheets of Figure 2.4.4-1. Seasonally varying storage allocations in the major projects are shown in the eleven sheets of Figure 2.4.1-6.

There are no current plans to construct dams and reservoirs that could adversely affect flood levels at the CRN Site.

2.4.4.2 Dam Failure Permutations

The discussion of dam failure permutations has been separated into three-subsections—Seismic Failure Analysis (2.4.4.2.1), Hydrologic Failure Analysis (2.4.4.2.2), and Failure by Other Methods Analysis (2.4.4.2.3).

2.4.4.2.1 Seismic Failure Analysis

Interim Staff Guidance for Assessment of Flooding Hazards Due to Dam Failure (JLD-ISG-2013-01, Reference 2.4.4-1) from the NRC recommends a dam should be assumed to fail if it cannot withstand the relevant seismic hazards (e.g., vibratory ground motion at spectral frequencies of importance, fault displacement, loss of strength) with an annual exceedance probability of 1×10^{-4} per year. JLD-ISG-2013-01 also provided guidance in modeling the consequences of seismic dam failure. If a dam fails under the 1×10^{-4} annual exceedance probability seismic hazard, the seismic failure is assumed to coincide with the peak water level from a 25-yr flood. If a dam fails under one-half of the 1×10^{-4} annual exceedance probability seismic hazard, the seismic failure is assumed to coincide with the peak water level from a 500-yr flood.

Concrete Section and Earthen Embankment Stability Analysis

There are eleven major dams that can influence the CRN Site flood levels—two on the Clinch River and nine on the Tennessee River system upstream of Watts Bar Dam. These were examined individually and in combinations to determine if failure might result from a seismic event and if so, would failure concurrent with storm runoff create maximum flood levels at the CRN Site.

Of the eleven major dams examined, global stability of the concrete dam and earthen embankment sections was analyzed for the maximum normal pool headwater/tailwater levels in combination with two seismic events: (1) 1 x 10^{-4} annual exceedance probability seismic hazard and (2) one-half of the 1 x 10^{-4} annual exceedance probability seismic hazard. Final stability conclusions were based on current TVA acceptance criteria (Reference 2.4.4-4) for the post-earthquake condition.

Spillway Gate Failures

(SRI/CEII) During seismic conditions, the spillway gates of [redacted] were assumed to fail with the failure of the spillways. For conservatism [redacted] and its spillway gates were assumed not to fail.

Lock Gates

(SRI/CEII) Of the dams above Watts Bar Dam which influence flood levels at the CRN Site, two of the dams, [redacted] Dam and [redacted] Dam, have locks and lock gates (see Subsection 2.4.1). The lock gates at [redacted] Dam were assumed to fail during seismic simulations with the failure of the lock. The lock gates at [redacted] Dam were assumed not to fail during seismic simulations. If the [redacted] lock gates should fail in the seismic event, the impact at the CRN Site is not significant.

Embankment Failure Considerations

Consistent with the JLD-ISG-2013-01 (Reference 2.4.4-1), the embankment was first subjected to the two seismic events combined with normal pool. The embankments were then checked for stability post-earthquake based on the post-earthquake conditions. Conventional limit equilibrium methods of slope stability analysis are used to investigate the equilibrium of a soil mass tending to move downslope under the influence of gravity. The analyses were performed by reducing the shear strengths to reflect post-earthquake conditions. The acceptable post-earthquake factor of safety is 1.1. If the factor of safety is less than 1.1, the embankment may still have acceptable seismic stability provided that estimated deformations are less than two feet and the amount of deformation is less than half the filter widths.

(SRI/CEII) The embankment outside of the acceptance criteria and postulated for failure within the model was at [redacted] Dam (during a 10,000-yr seismic event). Evaluated embankment portions of the remaining dams, including [redacted] Dams, were concluded to be stable during a half-10,000-yr or 10,000-yr seismic event. The main embankment of [redacted] Dam could fail during both the half-10,000-yr and 10,000-yr seismic events. However, for conservatism, [redacted] Dam was assumed not to fail which would result in a higher water surface elevation at the CRN Site.

Seismic Dam Failure Combination

(SRI/CEII) The half-10,000-yr Douglas centered seismic event in combination with a 500-yr June flood event includes seismic failures of [redacted] Dams as well as seismic failures on downstream tributaries including [redacted], and [redacted]. The 10,000-yr Fort Loudoun centered seismic event in combination with a 25-yr June flood event includes seismic failures of [redacted] Dams as well as seismic failures on downstream tributaries including [redacted] were not analyzed for these seismic events and were assumed to fail in these combinations. It was assumed that [redacted] Dam would not fail in order to maximize the water surface elevation upstream at the CRN Site. [redacted] Dam, upstream of the

(SRI/CEII) CRN Site, was evaluated for stability for the [redacted] Dam site-specific 10,000-yr and half-10,000-yr seismic events. [redacted] Dam was determined to be stable post-seismically at the normal maximum pool; therefore, a scenario that included a seismically induced failure of [redacted] Dam was not warranted.

Flood Routing

Flood inflow hydrographs were developed by using watershed gaged data to scale prototypical inflow hydrographs to meet estimated 25- and 500-year volume targets.

Guidance for development of probabilistic point rainfall estimates is published in Reference 2.4.4-11. Reference 2.4.4-11, Section 5, indicates point rainfall estimate data represents rainfall frequency at a point approximately 0.5-miles square and is not directly applicable for larger areas. Reference 2.4.4-12 states that point estimates may be applied to larger areas after adjustment through the use of Areal Reduction Factors (ARFs) for areas up to 400 sq mi. Watersheds impacting the Clinch River Nuclear (CRN) Site are 17,310 sq mi above Watts Bar Dam and 3382 sq mi above the CRN Site. Because these areas are significantly beyond the published limits for ARFs, the application for ARF adjusted point rainfall based on Reference 2.4.4-11 was judged not suitable. Therefore, an alternate methodology for production of scaled inflow hydrographs was developed to meet the requirements. This methodology uses historical gaged data across the watershed above the Watts Bar Dam aggregated into annual maximum series for 1- to 5-day durations to estimate 25- and 500-year frequency stream flows.

TVA has maintained Estimated Local Flow (ELF) data at gaged points in the Tennessee River watershed since 1903. These data represent inflows at the referenced gage point and are independent of river regulation. The daily data from 1903 through 2013 were compiled into 'X'-day values representing the corresponding durational flows (in cfs per 'X' days) for incremental daily durations of 1 to 5 days. The daily average for the 'X'-days were centered on each date for the odd durations and even durations were calculated using the average based on the leading center day. The series data were checked for conflict between same 'X'-day duration water years to identify and eliminate any overlapping events at the end of one water year and the beginning of the subsequent year. Conflicts were resolved by keeping the larger of the two series values and selecting the next highest non-overlapping annual value for the lower value water year. The 'X'-day data sets were arranged by water year (October 1 – September 30) and the annual maximum values for each duration for each water year were identified.

Following the guidance of Reference 2.4.4-8, an annual duration series (yearly 'X'-day maximum) was developed for each 'X'-day duration data set. A log-Pearson Type III distribution was applied to the resulting annual series following the methodologies described in References 2.4.4-8 and 2.4.4-10. Correction for data skew and elimination of low and high outliers were performed on the final distribution. A 10 percent significance level K value was used for the outlier check per guidance in Reference 2.4.4-8, Appendix 4. The resulting distributions provide both the 25- and the 500-year 'X'-day durational average streamflows. Because the resulting streamflows represent average flows over the respective duration, the estimates were used as streamflow volumes (i.e. durational streamflow x respective duration). The durational volumes above the Watts Bar project watershed were then selected as the target values for adjustment of the prototype inflow hydrographs.

The prototype inflow hydrographs are a representative storm event using published National Weather Service Atlas 14 data. A 25-year point rainfall at the centroid of the watershed above Chickamauga Dam was selected as the prototype rainfall for the watershed. A uniform rainfall areal distribution was applied over all sub-basins with a temporal distribution placing the peak rainfall according to a World Curve approach for a 24-hour event (Reference 2.4.4-9). Rainfall was applied with losses using the NRCS curve number methodology with validated curve

numbers for the season, and baseflows applied were June average monthly values. Runoff transformation was accomplished by manual spreadsheet convolution using validated sub-basin unit hydrographs (UHs). Resulting inflow hydrograph data were multiplied by scaling factors applied to all sub-basins to achieve the target volumes for the 25-yr and 500-yr events at each daily duration from 1 to 5 days. Adjustment ratios at the maxima were varied iteratively to achieve an acceptable difference in volume between the targets and the final summed hydrographs for the 1- through 4-day values. The 5-day volume target was included in order to maintain an acceptable slope between the 4th and 5th day maxima which made the adjustment to meet the 4-day volume more reasonable. However, the 5-day maximum ratio tended to be very high since the applied rainfall was a 4-day event with losses. This 5-day ratio generated hydrograph ordinates that were considered to be artifacts. However, the volumes met the target values and were judged reasonable. Additionally, time steps more than 1 day after the 4-day peak ordinate applied a recession constant of 10 percent per day to the ratio values to smooth the falling limb and minimize ratio generated artifacts. The final hydrograph ordinates were summed and volumes calculated to confirm that the target volumes had been met or exceeded. The adjusted surface runoff values were limited to be no smaller than the constant baseflow.

During postulated single and multiple project failure events, the concurrent failure of National Inventory of Dams (NID) identified projects, as discussed in Subsection 2.4.3.4.1, outside the model is considered possible. The NID volumes are located across the sub-basins with conveyances having differing sinuosity, length, slope, cross-sectional and roughness characteristics. As a result, the postulated failure waves are expected to pass through a variety of supercritical, critical and subcritical flow regimes as they traverse the respective reaches, starting at the failure location and ending at the respective model input points. The resulting translation reduces the peak flows and spreads the time base of the volume input. A simplified calculation approach was used to account for the NID volumes under these failure conditions. A time to peak of 20 minutes was assumed for the failure hydrographs. A Froehlich approach was used to postulate the individual failure hydrograph peak flows. The individual hydrographs were then combined into a composite triangular hydrograph based on distance of the NID projects from the model, and the peaks were adjusted to preserve volume ensuring that the entire NID volume was included in the failure flows (Figures 2.4.4-5, 2.4.4-6, and 2.4.4-7).

The runoff model described in Subsection 2.4.3.4 was used to evaluate the potentially critical seismic events involving dam failures above the plant. Reservoir operating procedures used were those applicable to the season and flood inflows.

Based on a review of the flood elevations at the Watts Bar Dam in the half-10,000-yr seismic event compared to the 10,000-yr seismic event, the half-10,000-yr seismic event was determined to be controlling. The seismic dam failure combination producing the most critical elevation at the CRN Site is the half-10,000-yr Douglas centered seismic event during a 500-yr June flood event.

2.4.4.2.2 Hydrologic Failure Analysis

Upstream and downstream dams, which could have a significant influence on flood levels at the CRN Site, were examined for potential failure during the PMF. Concrete sections were examined for overturning and for horizontal shear failure with a resultant sliding of the structures. Spillway and lock gates were examined for stability at potentially critical water levels, and against failure from being struck by waterborne objects. Concrete lock structures were examined for stability, and earth embankments were examined for stability as well as erosion due to overtopping.

Concrete Section and Earthen Embankment Stability Analysis

For concrete dam and earthen embankment sections, global stability was analyzed for the headwater/tailwater levels that would occur in the PMF using TVA current acceptance criteria

(SRI/CEII) (Reference 2.4.4-4). The concrete dams that were outside of this acceptance criteria were postulated for failure within the model if a critical elevation was reached. For Watts Bar Dam and dams upstream, those assumed to fail at critical reservoir elevations are [redacted]. Dams without updated stability calculations and assumed to fail in the PMF included [redacted]. Concrete portions of [redacted] Dam could also fail if the headwater reached a critical elevation. However, for conservatism, [redacted] Dam was assumed not to fail, resulting in a higher water surface elevation at the CRN Site. [redacted] Dam, upstream of the CRN Site, was evaluated for stability for the maximum PMF headwater/tailwater conditions and determined to be stable.

Spillway Gate Failures

During peak PMF conditions, the radial spillway gates of Watts Bar Dams are modeled as fully open. The spillway gates are conservatively assumed not to fail because spillway gate failure would reduce the flood elevation at the CRN Site.

A sensitivity analysis for spillway gates that are inoperable and closed as well as potential for spillway gate blockage due to debris was performed and described in Subsection 2.4.3.4.

Lock Gates

(SRI/CEII) Of the dams which influence flood levels at the CRN Site, Watts Bar, Melton Hill and Fort Loudoun Dams have locks and lock gates (see Subsection 2.4.1). The lock gates at Fort Loudoun Dam and Watts Bar Dam were examined with the conclusion that no potential for failure exists. The lock gate structural elements may experience localized yielding and may not function normally following the most severe headwater/tailwater conditions. Because [redacted] Dam was overtopped and assumed to fail totally during the PMF analysis, its lock gates were not examined.

Embankment Breaching

For embankment dam sections, global stability was analyzed for the maximum headwater and corresponding tailwater levels that would occur in the PMF. Conventional limit equilibrium methods of slope stability analysis were used to investigate the equilibrium of a soil mass tending to move downslope under the influence of gravity. Comparisons were made between forces, moments, or stresses tending to cause instability of the mass and those that resist instability.

(SRI/CEII) The PMF could overtop and subsequently breach [redacted] at [redacted]. A breach at these dams could add to PMF elevations. Additionally, the [redacted] could fail if the headwater reached a critical elevation. However, for conservatism, the [redacted] was assumed not to fail resulting in a higher water surface elevation at the CRN Site.

The Von Thun and Gillette method was selected as the appropriate method to determine the breach characteristics of an embankment breach. In the event that a breach was larger than the cross-section of the channel at the location of the embankment, a total failure of the embankment was postulated.

Von Thun and Gillette (Reference 2.4.4-5) proposed the average breach width of an embankment section as defined by:

$$B_{Avg} = 2.5 \times h_w + C_b$$ Equation 2.4.4-1

Where B_{Avg} = average breach width (ft), h_w = depth of water at the dam at the time of failure (ft), and C_b is a function of reservoir storage, or 180 ft (for reservoirs above 10,000 ac-ft). B_{Avg} occurs at the elevation corresponding to one-half of the dam height, H_d.

The shape of the breach was trapezoidal with 1:1 (horizontal:vertical) side-slopes, and the total flow through the breach was calculated in two components: the rectangular portion and the slope portion. The limit of the rectangular portion was the base of the breach extended vertically to the water surface. The slope portion of the breach consisted of the triangles on either side of the rectangle extended to the water surface. The total flow was found by the following equation:

$$Q_{total} = Q_{rectangle} \times Q_{slope}$$ Equation 2.4.4-2

The flow through a rectangular weir was found with the following equation:

$$Q_f = C_f \times L \times H_c^{1.5}$$ Equation 2.4.4-3

In which Q_f = free discharge over rectangular weir (cfs), C_f = free discharge coefficient ($t.^{0.5}$/s, may vary with HW), L = length of the horizontal portion of the overflowing section (ft), H_c = head on crest (ft) = HW - Z_c, HW = headwater elevation (ft), and Z_c = crest elevation of overflowing section (ft).

This equation was modified to account for tailwater submergence as follows:

$Q_{fs} = Q_f S_f$ Equation 2.4.4-4

In which Q_{fs} = corrected free discharge (cfs) and S_f = tailwater submergence factor (dimensionless, varying between 0 and 1). S_f varied with d/H_c where d = TW - Z_c (ft) and TW = tailwater elevation (ft).

The weir length, L (ft) of the rectangular portion of the breach (the bottom width of the trapezoid) was found as follows:

L = B_{Avg} – [(Elevation of B_{Avg} on right side of breach – Elevation of base of breach) x z + (Elevation of B_{Avg} on left side of breach – Elevation of base of breach) x z]

Where z was the horizontal distance per vertical foot of side slope. For the sloped portion of the breach, the discharge through each sloped side of the trapezoid, Q_{slope} (cfs), was found through the weir equation where:

L_{slope} was the length of weir (ft), found by the following equation:

$L_{slope} = F_w \times H_d \times z$ Equation 2.4.4-5

In which H_d was the height of the dam (t.), and F_w was the wet fraction, defined by the percentage of wetted perimeter of the sloped section. The wet fraction did not exceed a value of one and was defined by:

$$F_w = H_c/H_d$$ Equation 2.4.4-6

If $H_c \leq H_d$, $H_{c\ slope}$ was the average value of head over the slope and was found by the following:

$H_{c\ slope} = ½ \times H_c$ (Figure 2.4.4-2) Equation 2.4.4-7

If $H_c > H_d$, $H_{c\ slope}$ was the average value of head over the slope and was found by the following:

$H_{c\ slope} = ½ \times H_d + (H_c - H_d)$ (Figure 2.4.4-2) Equation 2.4.4-8

In order to calculate the submergence effects on the sloped portion, the average tailwater level over the sloped portion of the breach, d, was calculated. The calculated difference between the headwater elevation (HW) and H_c for the sloped portion was subtracted from the tailwater elevation (TW). d/Hc for the sloped portion is calculated with the following equation:

$$d/_{H_{c\ slope}} = \frac{TW - (HW - H_{c\ slope})}{H_{c\ slope}}$$ Equation 2.4.4-9

The length of the failed section of the dam, T (ft), was considered to be the top width of the failed trapezoidal section. This was found by the following equation:

$T = B_{Avg}$ + [(Elevation of Intact Emb Crest - Elevation of B_{Avg} - right of breach) x z + (Elevation of Intact Emb Crest - Elevation of B_{Avg} left of breach) x z] Equation 2.4.4-10

The length of intact portion of the dam, L_{Intact} (ft), was the difference between the total length and the failed length.

$L_{Intact} = L_{dam} – T$ Equation 2.4.4-11

Where, L_{dam} was the total length of the dam (ft)

(SRI/CEII) In the case of [redacted] Dam, a Von Thun and Gillette breach was assumed if the embankments were overtopped. In the case of [redacted]. For the controlling PMF the [redacted] saddle dams were assumed to fail with a Von Thun and Gillette breach. A total embankment failure was assumed for [redacted]. A total failure of [redacted] was assumed. [redacted] nd [redacted] Dams were not overtopped in the controlling PMF and therefore not assumed to fail.

2.4.4.2.3 Failure by Other Methods Analysis

(SRI/CEII) A sunny day failure of [redacted] Dam, upstream of the CRN Site, has the potential to influence site flood levels. The most likely [redacted] Dam failure under sunny day conditions would be the [redacted]

(SRI/CEII) [redacted] Dam. The failure of [redacted] Dam could result in a subsequent overtopping failure of [redacted] Dam, producing a peak water surface elevation of [redacted] ft National Geodetic Vertical Datum of 1929 (NGVD29) at the CRN Site.

The controlling PMF event at the CRN Site, with 100 percent runoff, results in overtopping dam failures that bound any site-specific events that would result in an overtopping dam failure.

2.4.4.3 Unsteady Flow Analysis of Potential Dam Failures

The unsteady flow runoff and stream course models described in Subsection 2.4.3.3 were used to evaluate the site flood levels from PMF events involving dam failures above the plant, from seismic dam failures above the plant, and from sunny day dam failures. Reservoir operating procedures used were those applicable to the season and flood inflows.

(SRI/CEII) The PMF event would overtop and breach [redacted] These are the only dams that would fail and they were assumed to fail instantaneously and either totally or as prescribed by the Von Thun and Gillette method. [redacted] Dam remained stable and [redacted] Dam was assumed not to breach to provide bounding backwater conditions at the CRN Site.

2.4.4.4 Water Level at CRN Site

The unsteady flow analysis described in Subsection 2.4.4.3 was performed for each of the dam failure permutation defined in Subsections 2.4.4.2.1, 2.4.4.2.2, and 2.4.4.2.3. The unsteady flow analysis provides the flow and peak still water levels at the CRN Site.

(SRI/CEII) As described in Subsection 2.4.3.2, the controlling PMF event at the CRN Site is the 7980 sq mi Bulls Gap centered March PMF. The resulting peak flow is 536,000 cfs and the peak water surface elevation is [redacted] ft NGVD29. The discharge and elevation hydrographs for the controlling PMF event are shown in Figure 2.4.3-3 and represent a point just upstream of the intake.

(SRI/CEII) Peak flow from the seismic failure analysis, the half-10,000-yr Douglas centered seismic event with a coincident 500-yr flood is 162,000 cfs and the peak water surface elevation is [redacted] ft NGVD29. The discharge and elevation hydrographs for the seismic failure analysis are shown in Figure 2.4.4-3 and represent a point just upstream of the intake.

(SRI/CEII) Peak flow from the sunny day failure of Norris Dam is 579,000 cfs and the peak water surface elevation is [redacted] ft NGVD29. The discharge and elevation hydrographs for the sunny day failure of Norris Dam are shown in Figure 2.4.4-4 and represent a point just upstream of the intake.

(SRI/CEII) A coincident 28 mph overland wind was applied resulting in a wave height of [redacted] ft from crest to trough. The maximum water surface elevation resulting from the combination of the controlling PMF storm, coincident hydrologic dam failures and windwave effects is [redacted] ft NGVD29. The impacts to the CRN Site from potential flood causing mechanisms have been evaluated. There are no impacts to safety-related systems, structures or components at the CRN Site.

2.4.4.5 Coincident Wind Wave

Wind waves to be associated with the PMF crest were computed using procedures of the USACE Coast Engineering Manual (Reference 2.4.4-6). Wind data from 2000 to the 2014 were

(SRI/CEII) collected at Huntsville, Alabama; Chattanooga, Knoxville, and Tri-Cities, Tennessee; and Asheville, North Carolina. The raw 2-minute average wind data were used to calculate the maximum 20-minute average wind speed for each year at each data collection site and the 2-yr wind speed was determined. The CRN Site overland wind speed of 28 mph was adjusted for overwater conditions resulting in an overwater wind speed of 33 mph. The effective fetch found for the CRN Site from available GIS terrain data was 4.25 mi, based on the site grade elevation of 821 feet North American Vertical Datum of 1988 (NAVD88), which results in the critical site fetch length (Figure 2.4.3-16). For a calculated 33 mph overwater 2-yr wind, the total wave height of [redacted] ft from crest to trough was calculated, which includes wave runup ([redacted] ft) and wave setup ([redacted] ft). When applied to the maximum water surface elevation discussed in Subsection 2.4.4.4, coincident wind wave results in a maximum water surface elevation of [redacted] ft NGVD29. CRN Site grade is 821 ft NAVD88(821.4 ft NGVD29), [redacted] ft higher than the maximum calculated water surface elevation with wind wave height. Because of the available margin, the coincident wind wave activity does not have an effect on flooding at the site.

2.4.4.6 Erosion and Deposition Effects

(SRI/CEII) The effects of the potential movement of erodible material with respect to flood levels at the CRN Site can be shown to be insignificant by taking a very conservative approach. If all of the earthen embankments and saddle dams postulated to fail in the bounding PMF simulation (also the simulation with the highest volume of breached material) were to be completely eroded and deposited downstream into Watts Bar Reservoir the resulting approximate 200,000,000 cubic yards of material would reduce the storage capacity of Watts Bar Reservoir by about 124,000 ac-ft (Reference 2.4.4-7). This is equivalent to less than a [redacted] foot rise in Watts Bar Reservoir with Watts Bar headwater elevation at the peak elevation of 777.3 ft NGVD29 during the bounding PMF simulation (Reference 2.4.4-7). This less than [redacted] foot rise in Watts Bar Reservoir is far short of the nearly 25 ft of elevation rise needed based on the bounding PMF results to reach preliminary CRN plant grade.

2.4.4.7 References

2.4.4-1. NRC, “Guidance for Assessment of Flooding Hazards Due to Dam Failure, Interim Staff Guidance,” Report JLD-ISG-2013-01, ADAMS Accession No. ML13151A153, Rev. 0, July 29, 2013.

2.4.4-2. ANSI/ANS-2.8-1992, “Determining Design Basis Flooding at Power Reactor Sites,” July 1992.

2.4.4-3. TVA, Division of Water Management, Geological Services Branch, “Southern Appalachian Tectonic Study,” Seay, William M., (ML082170494), Knoxville, Tennessee, January 1979.

2.4.4-4. *SRME - Design and Evaluation of New and Existing River System Dams*, SRME-SPP-27.001.

2.4.4-5. Von Thun, J. Lawrence, and David R. Gillette, *Guidance on Breach Parameters*, internal memorandum, U.S. Bureau of Reclamation, March 13, 1990.

2.4.4-6. U.S. Army Corps of Engineers, *Coast Engineering Manual,* EM1110-2-1100, Pts. 2 and 6.

2.4.4-7. BWSC, Inc., *Clinch River Nuclear Plant Sediment Transport Position Paper*, Rev. 0, January 20, 2015.

2.4.4-8. Guidelines for Determining Flood Flow Frequency, Bulletin #17B of the Hydrology Subcommittee, Interagency Advisory Committee on Water Data, Office of Water Data Coordination, Geological Survey, U.S. Department of the Interior, Revised September 1981 with March 1982 Editorial Corrections.

2.4.4-9. Moore, James N. and Ray C. Riley, “Comparison of Temporal Rainfall Distributions for Near Probable Maximum Precipitation Storm Events for Dam Design”, National Water Management Center, Natural Resources Conservation Service, (NRCS), Little Rock, Arkansas.

2.4.4-10. Hovey, Peter and Thomas DeFiore, “Using Modern Computing Tools to Fit the Pearson Type III Distribution to Aviation Loads Data”, Report # DOT/FAA/AR-03/62, Office of Aviation Research, Federal Aviation Administration, U.S. Department of Transportation, Washington, D.C., September 2003.

2.4.4-11. Bonnin, Geoffrey M., Deborah Martin, Bingzhang Lin, Tye Parzybok, Michael Yekta, David Riley, “NOAA Atlas 14, Precipitation-Frequency Atlas of the United States”, Volume 2 Version 3.0: Delaware, District of Columbia, Illinois, Indiana, Kentucky, Maryland, New Jersey, North Carolina, Ohio, Pennsylvania, South Carolina, Tennessee, Virginia, West Virginia, U.S. Department of Commerce, National Oceanic and Atmospheric Administration, National Weather Service, Silver Spring, Maryland, 2004, revised 2006.

2.4.4-12. Hershfield, David M., “Technical Paper No. 40 Rainfall Frequency Atlas of the United States for Durations from 30 Minutes to 24 Hours and Return Periods from 1 to 100 Years”, Department of Commerce, Cooperative Studies Section, Hydrologic Services Division for Engineering Division, Soil Conservation Service, U.S. Department of Agriculture; Washington, D.C. May 1961, Repaginated and Reprinted January 1963.

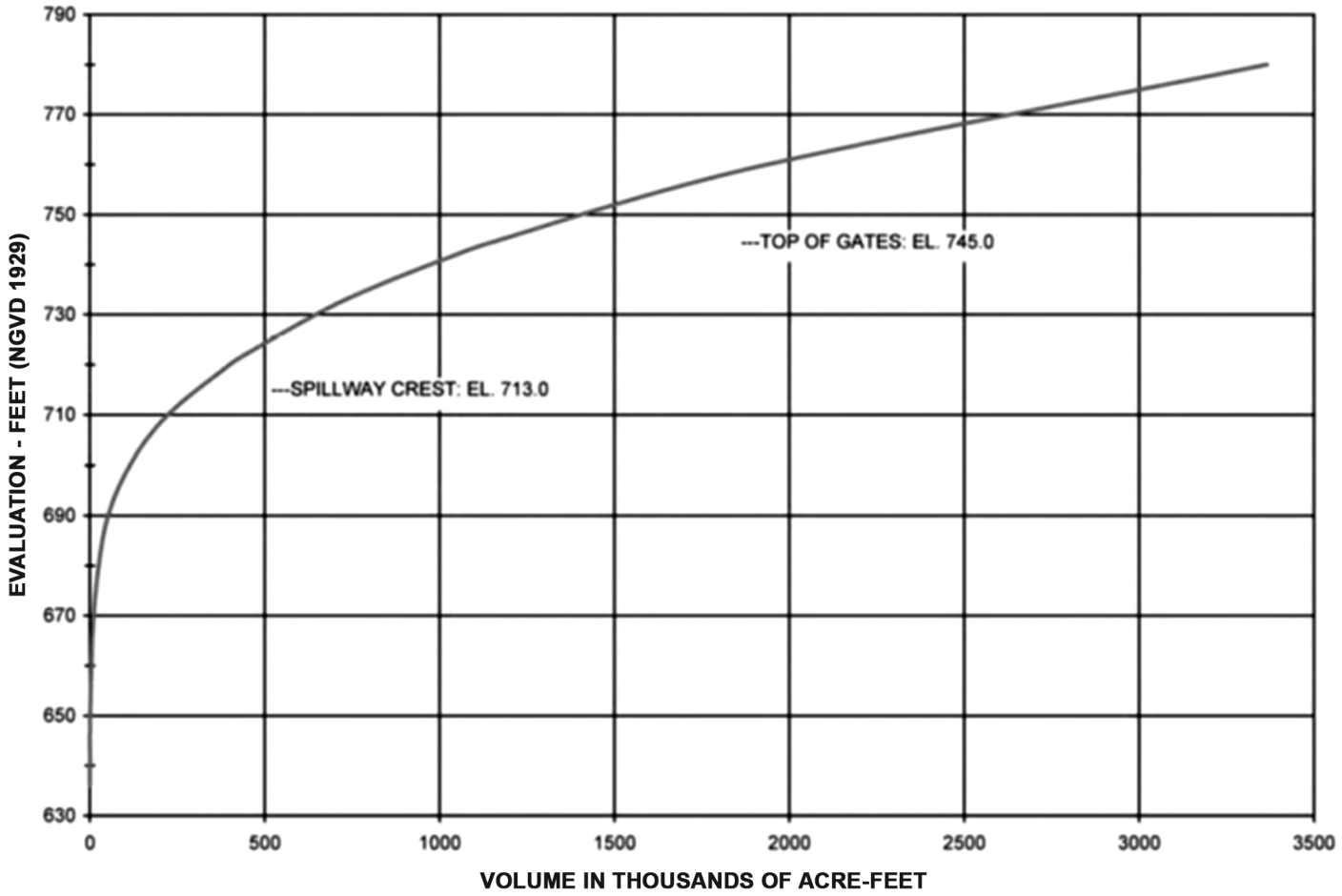

Figure 2.4.4-1. (Sheet 1 of 12) Reservoir Elevation-Storage Relationship, Watts Bar Reservoir

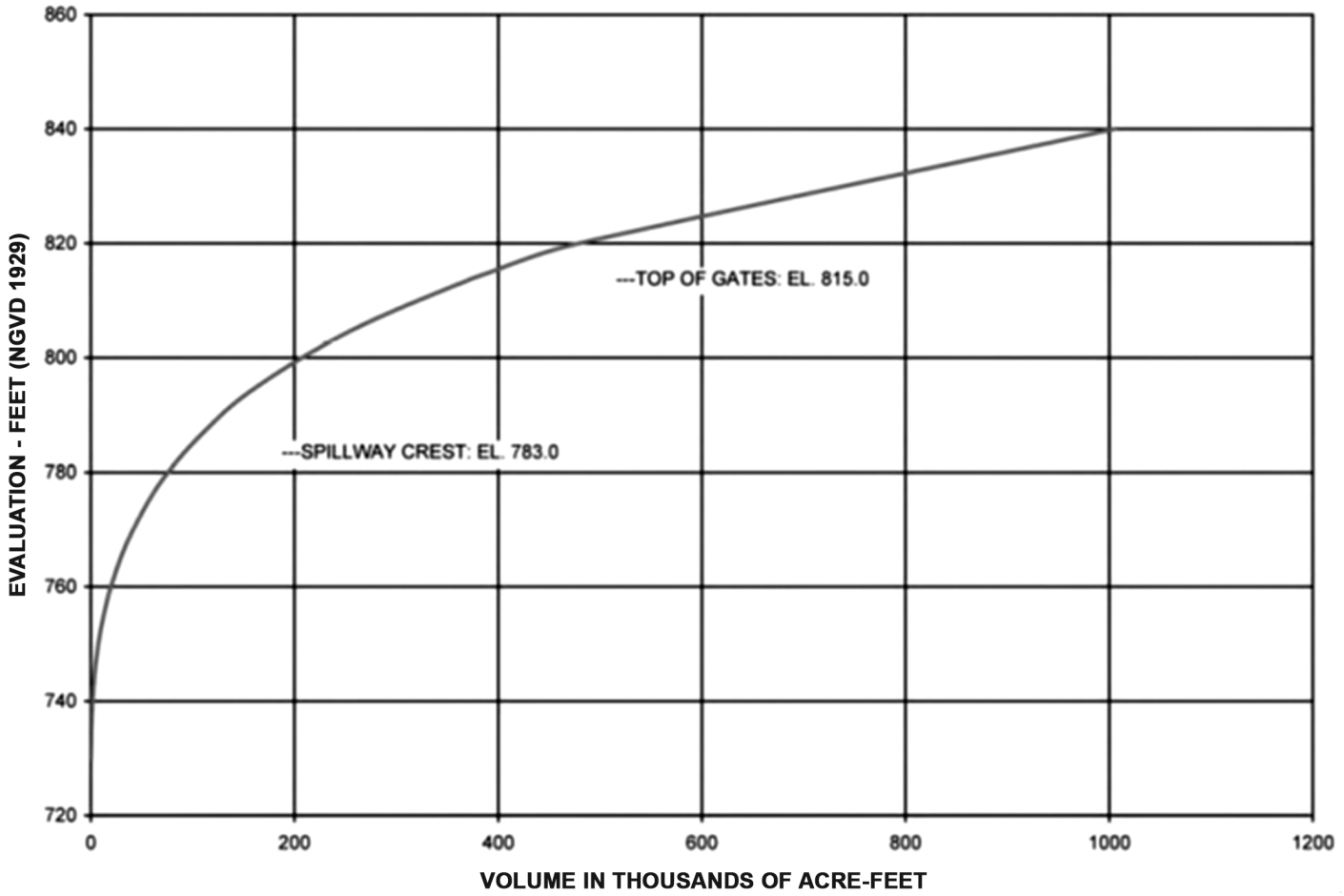

Figure 2.4.4-1. (Sheet 2 of 12) Reservoir Elevation-Storage Relationship, Fort Loudoun Reservoir

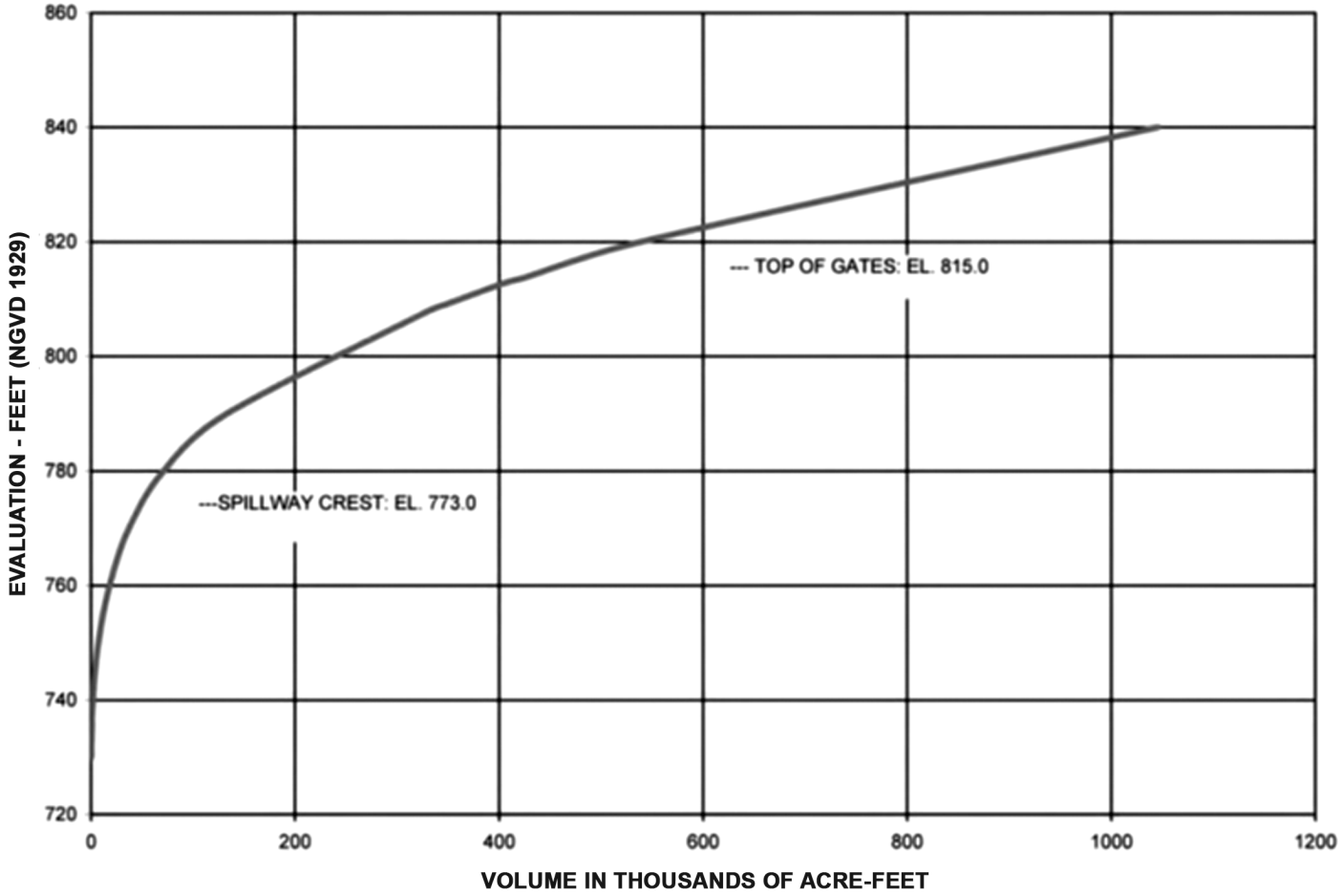

Figure 2.4.4-1. (Sheet 3 of 12) Reservoir Elevation-Storage Relationship, Tellico Reservoir

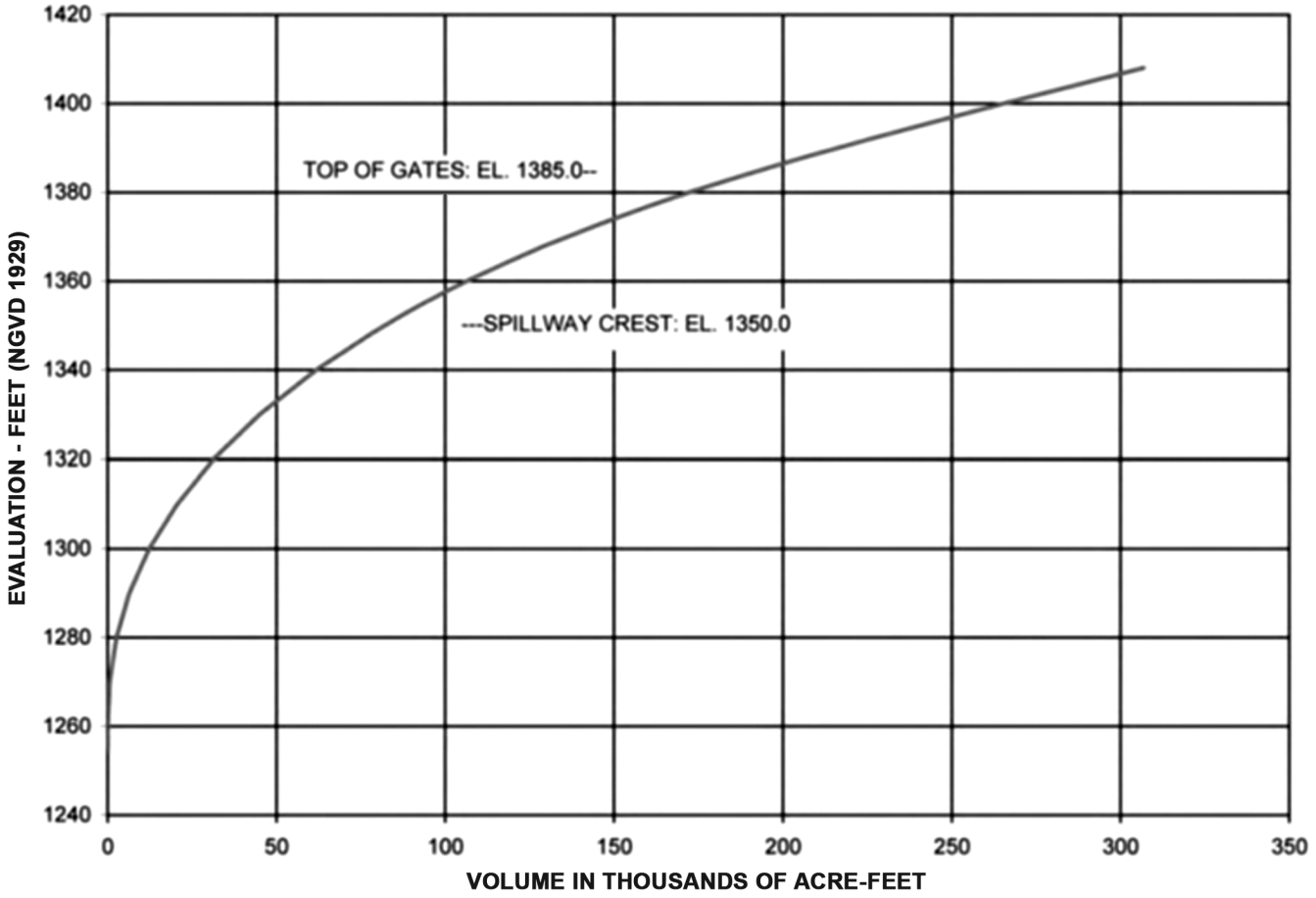

Figure 2.4.4-1. (Sheet 4 of 12) Reservoir Elevation-Storage Relationship, Boone Reservoir

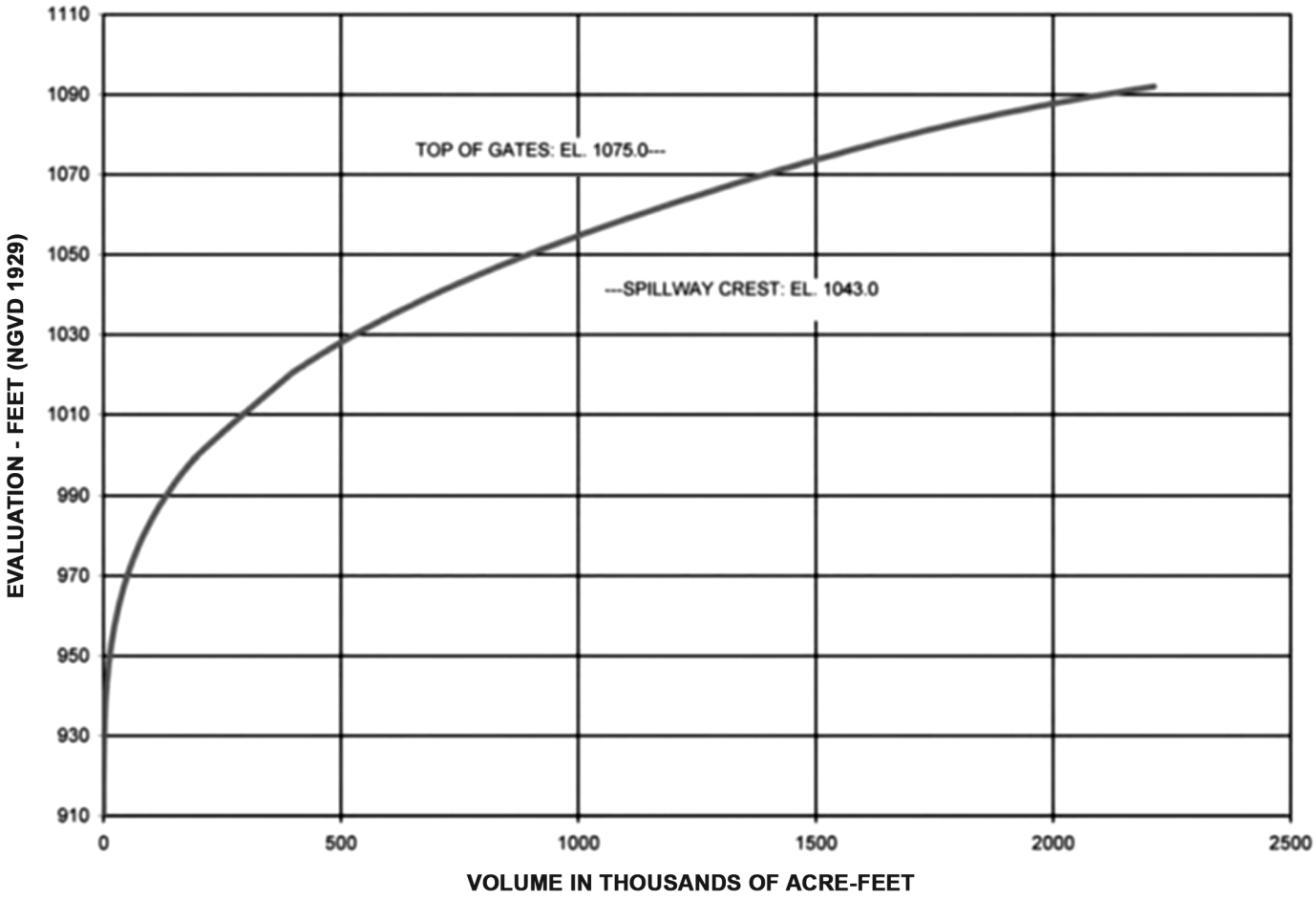

Figure 2.4.4-1. (Sheet 5 of 12) Reservoir Elevation-Storage Relationship, Cherokee Reservoir

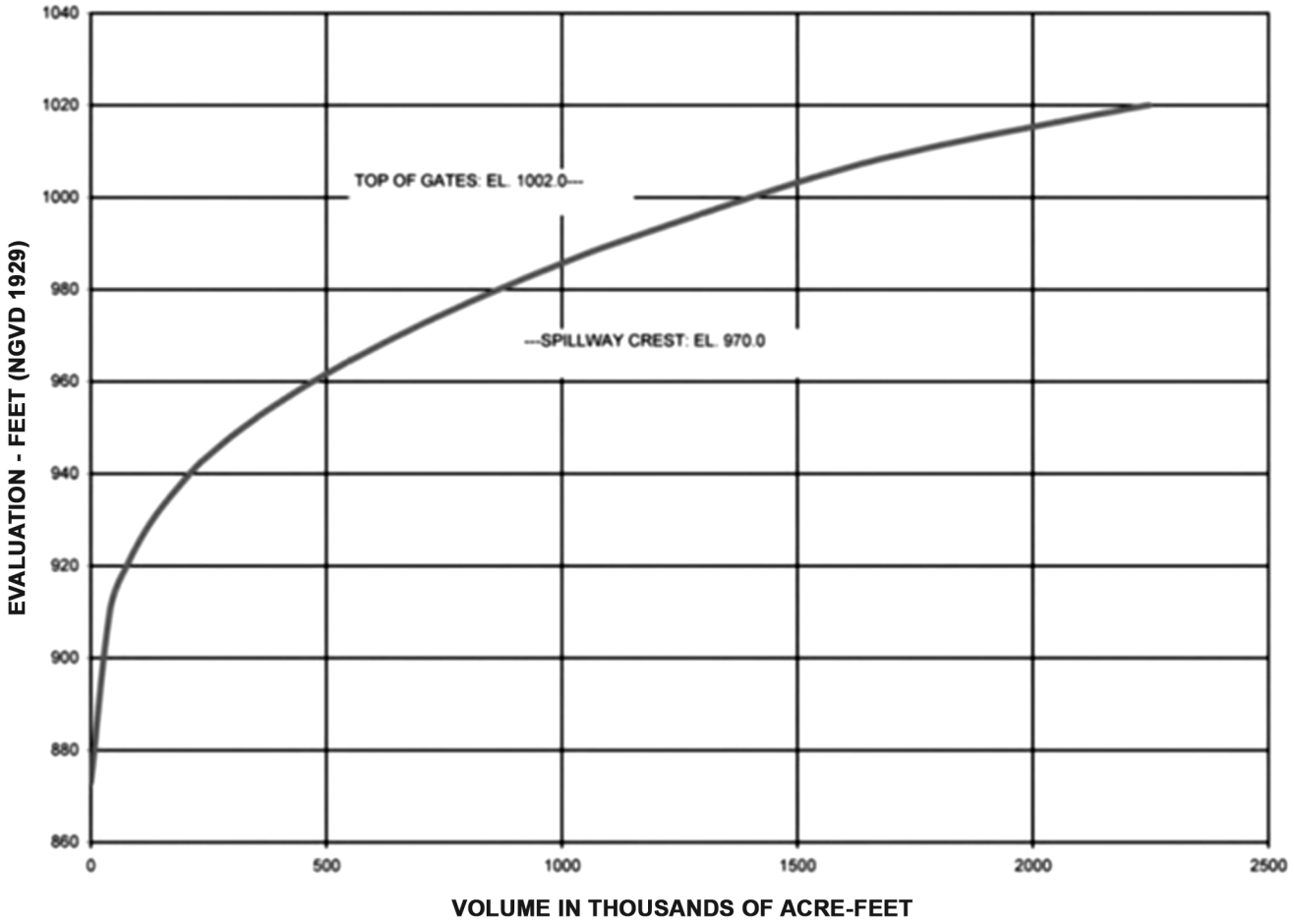

Figure 2.4.4-1. (Sheet 6 of 12) Reservoir Elevation-Storage Relationship, Douglas Reservoir

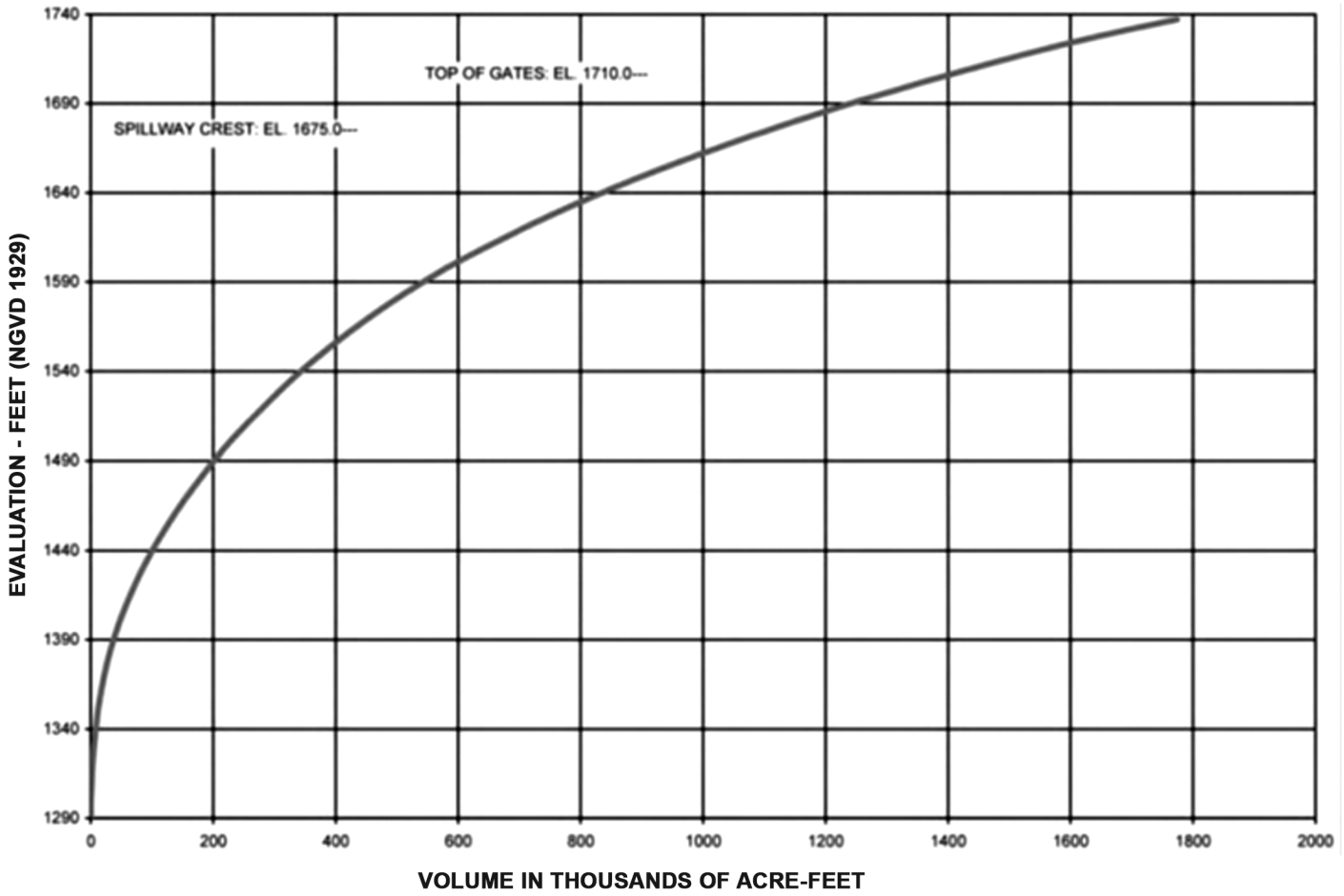

Figure 2.4.4-1. (Sheet 7 of 12) Reservoir Elevation-Storage Relationship, Fontana Reservoir

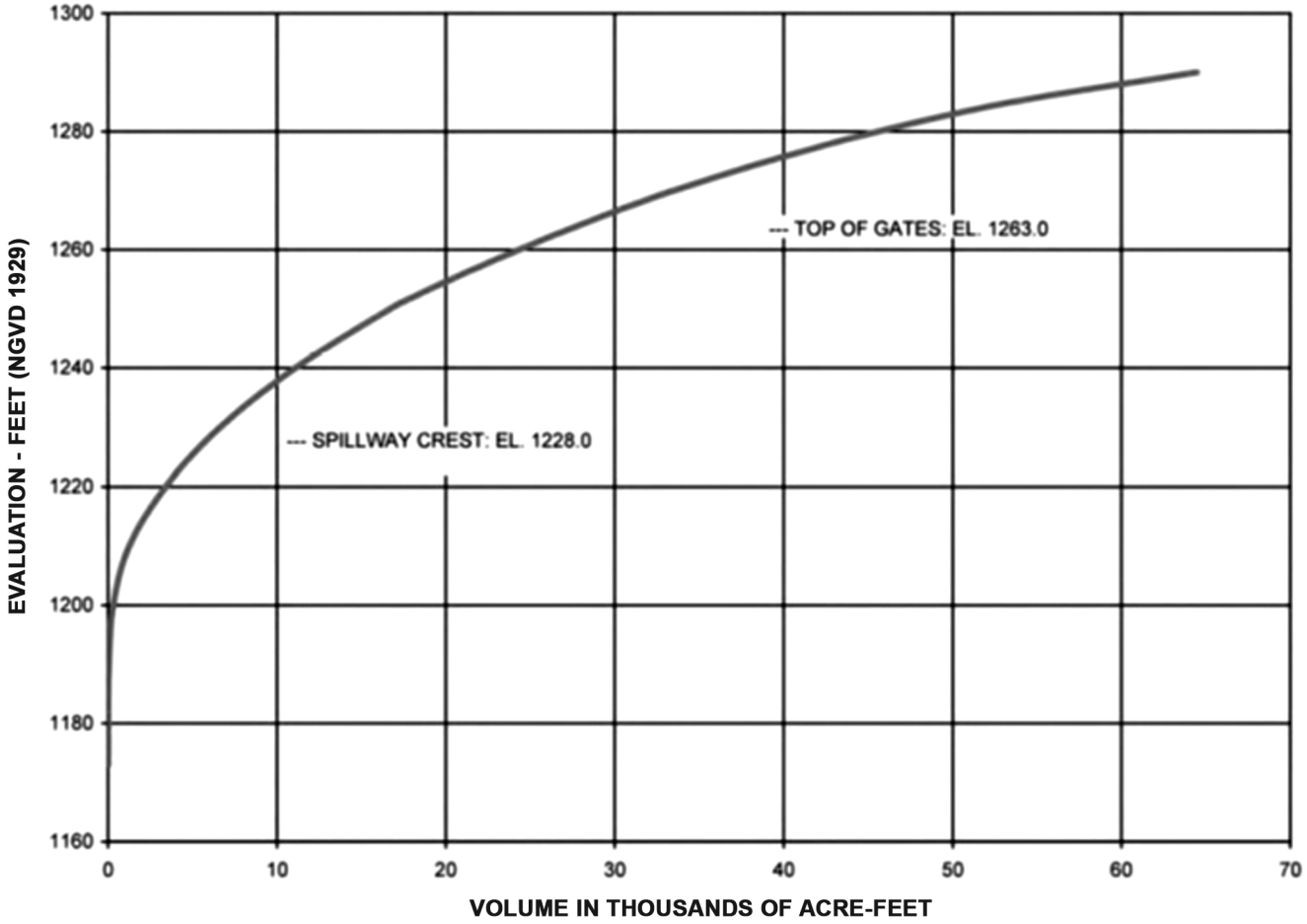

Figure 2.4.4-1. (Sheet 8 of 12) Reservoir Elevation-Storage Relationship, Fort Patrick Henry Reservoir

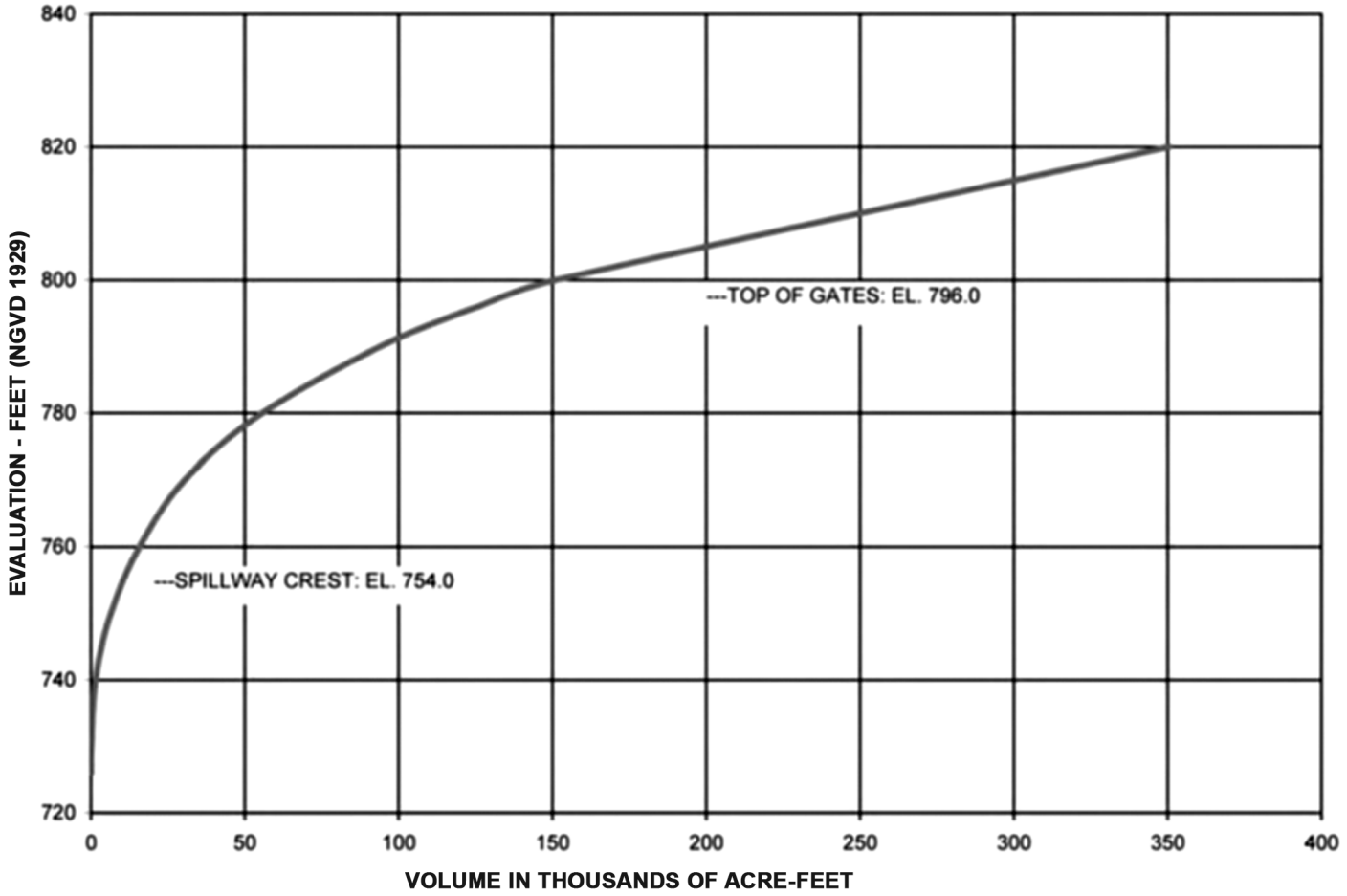

Figure 2.4.4-1. (Sheet 9 of 12) Reservoir Elevation-Storage Relationship, Melton Hill Reservoir

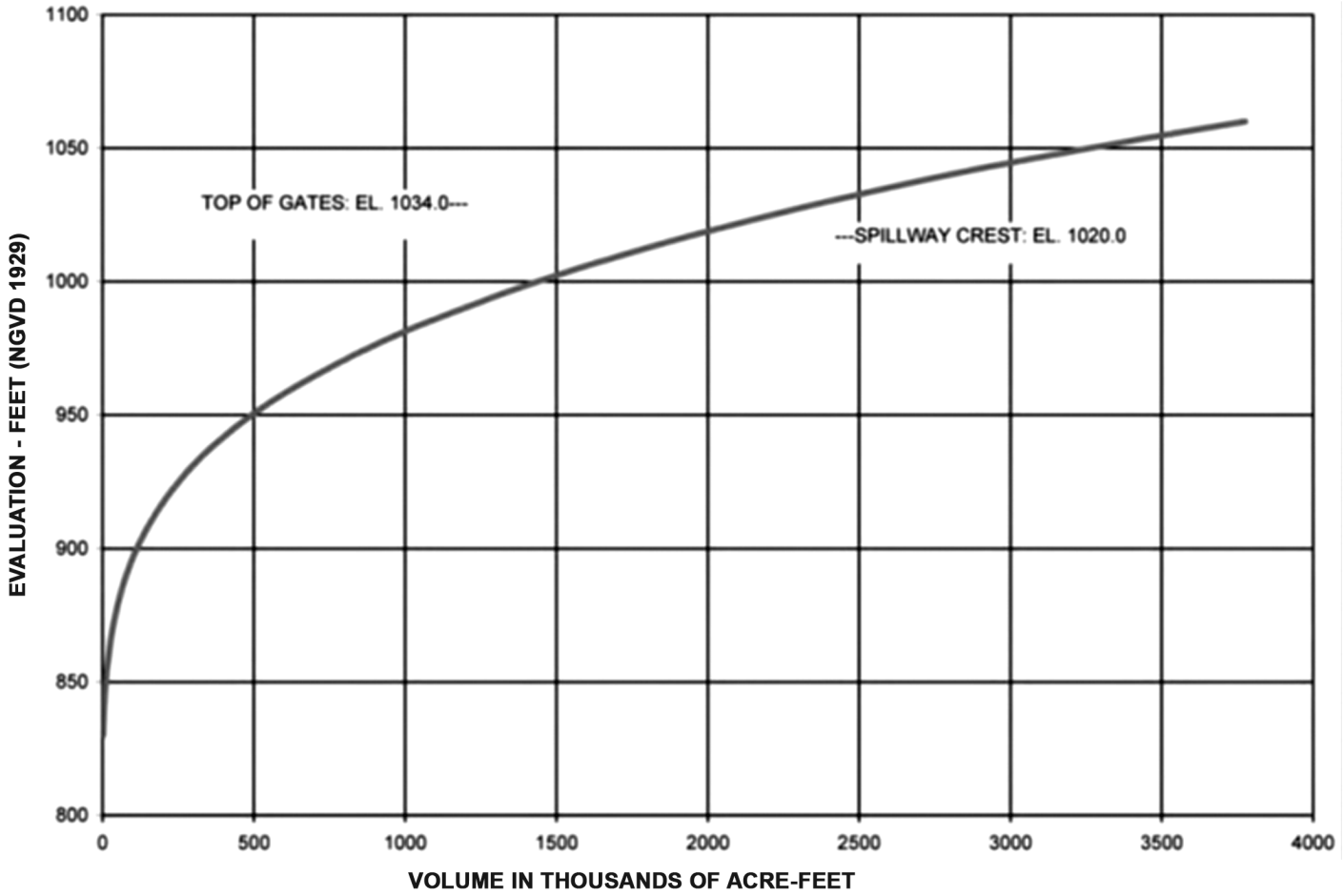

Figure 2.4.4-1. (Sheet 10 of 12) Reservoir Elevation-Storage Relationship, Norris Reservoir

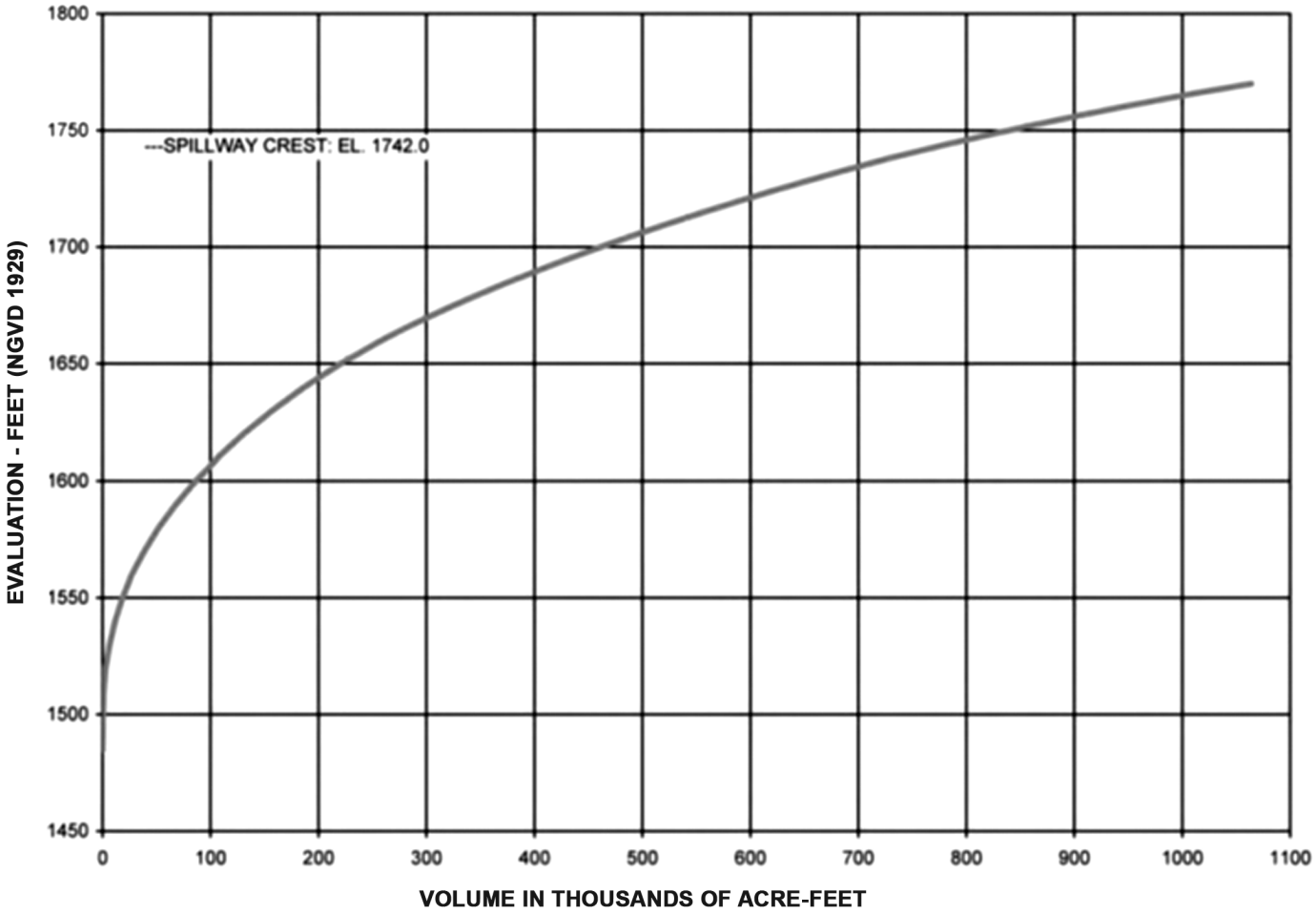

Figure 2.4.4-1. (Sheet 11 of 12) Reservoir Elevation-Storage Relationship, South Holston Reservoir

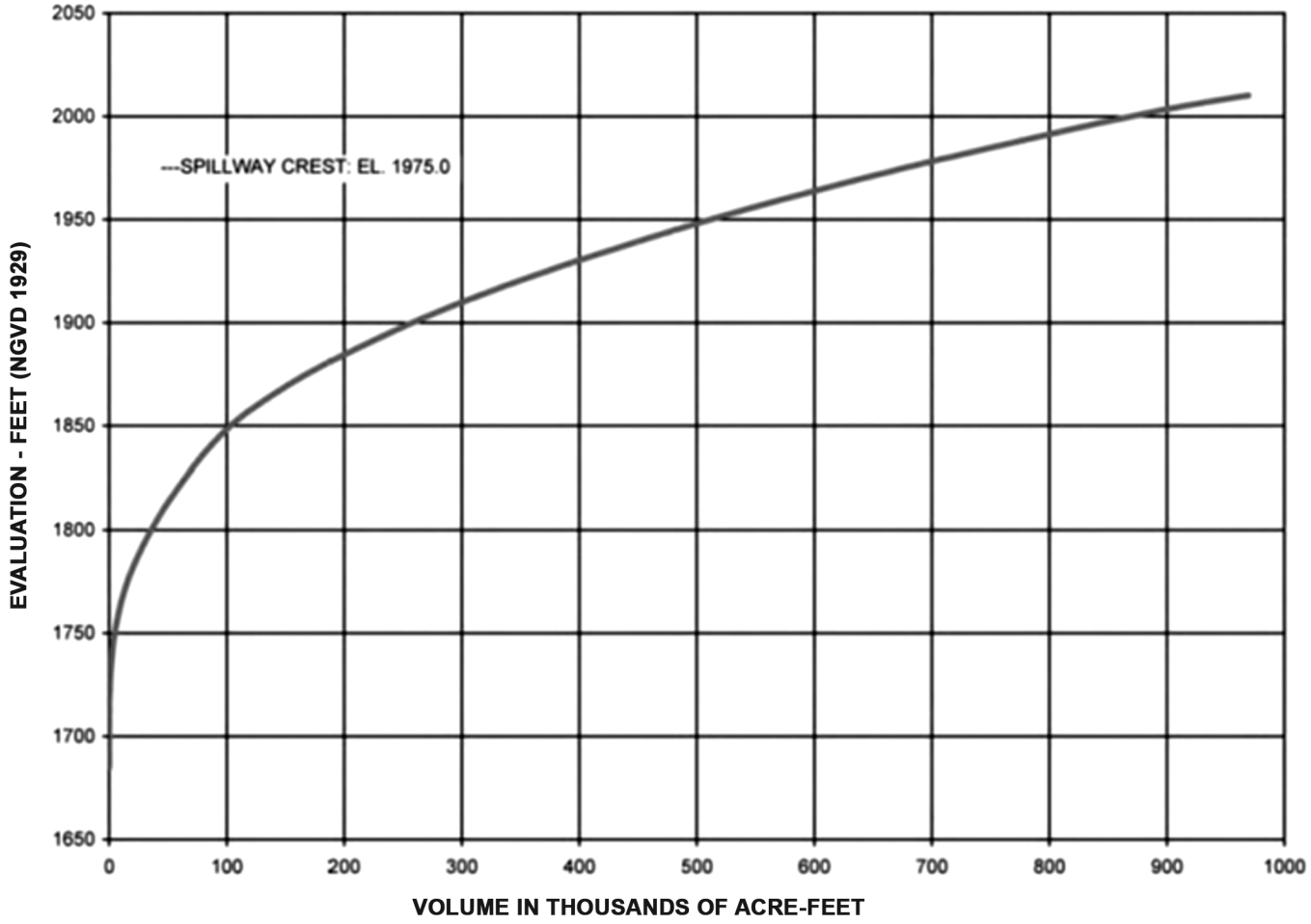

Figure 2.4.4-1. (Sheet 12 of 12) Reservoir Elevation-Storage Relationship, Watauga Reservoir

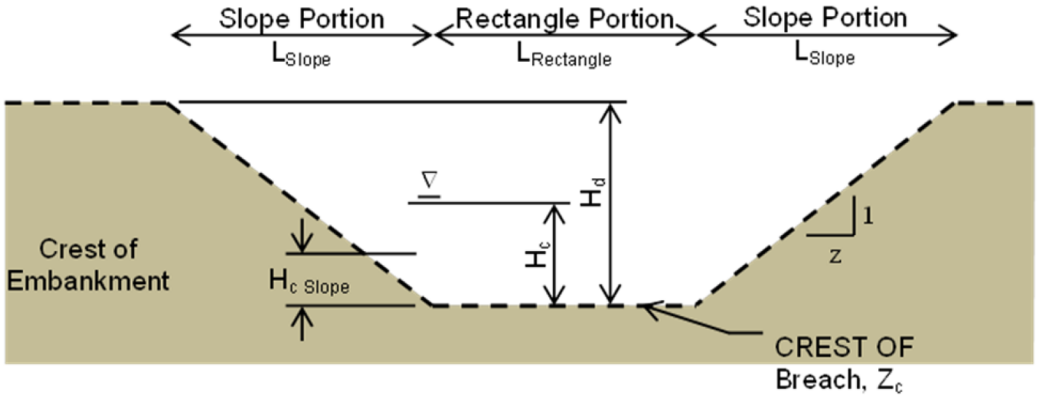

Diagram Illustrating the Head on Crest for the Rectangle and Slope Portions of a Breach Section when $H_c \leq H_d$

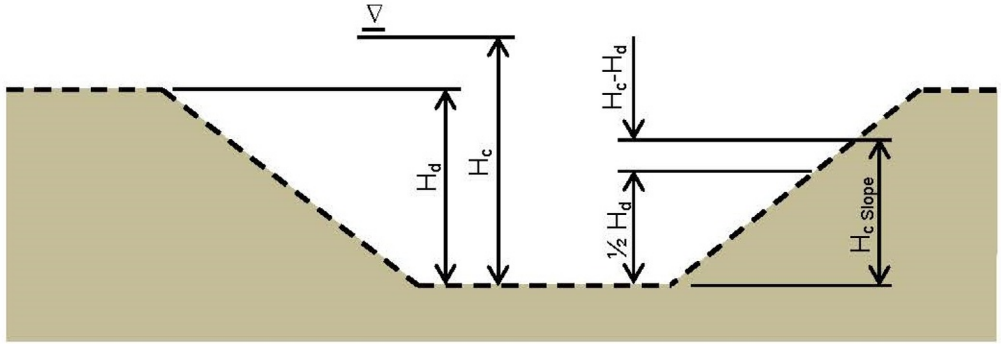

Diagram Illustrating the Head on Crest for the Rectangle and Slope Portions of a Breach Section when $H_c > H_d$

Figure 2.4.4-2. Head on Crest for the Rectangle and Slope Portions of a Breach Section

(SRI/CEII)

Figure 2.4.4-3. Elevation and Discharge Hydrograph at the Clinch River Nuclear Site from Seismic Dam Failure Analysis

(SRI/CEII)

Figure 2.4.4-4. Elevation and Discharge Hydrograph at Clinch River Nuclear Site from Sunny Day Dam Failure Analysis

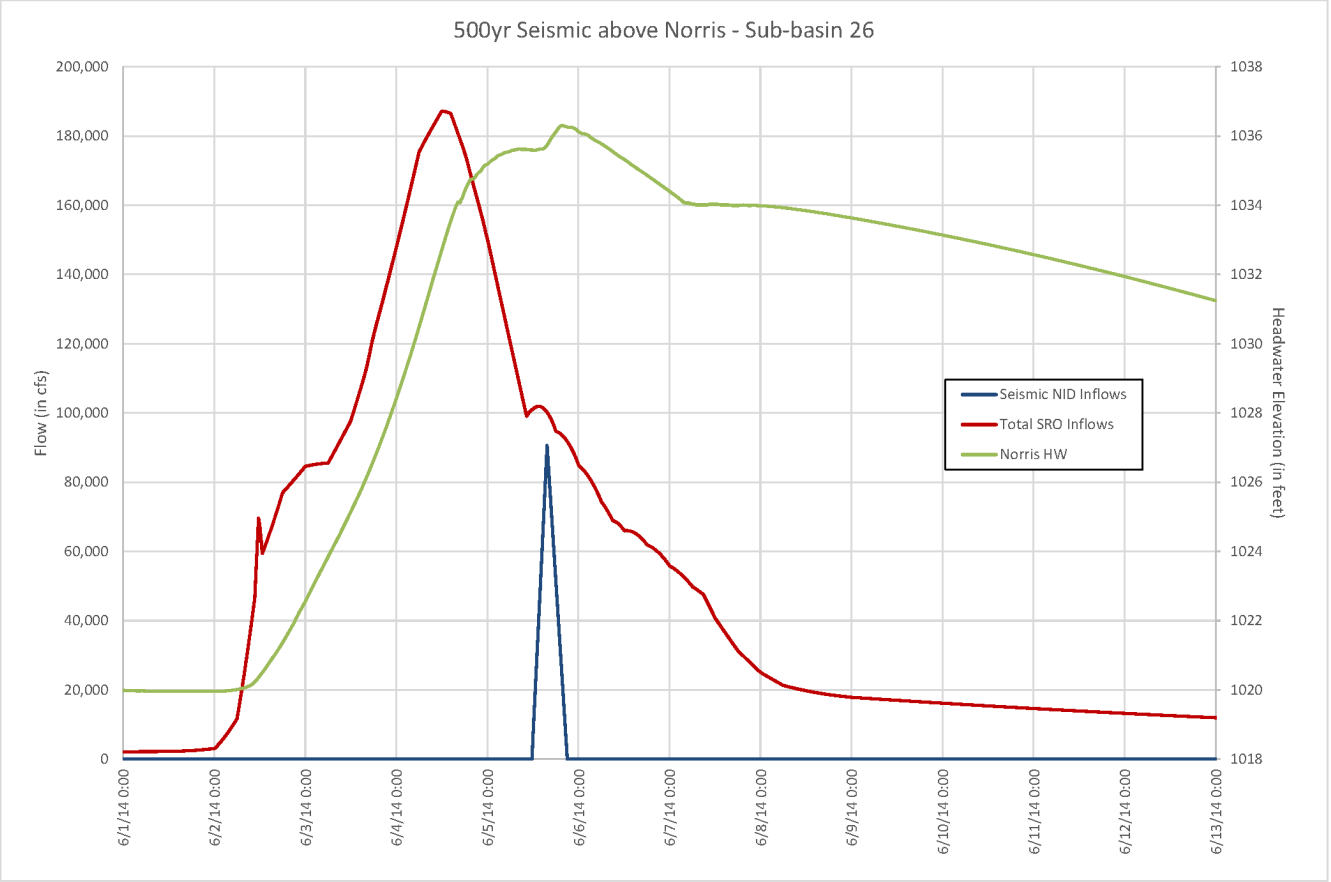

Figure 2.4.4-5. Seismic Inflow Hydrographs for 500-Yr June Flood Event – Norris Dam

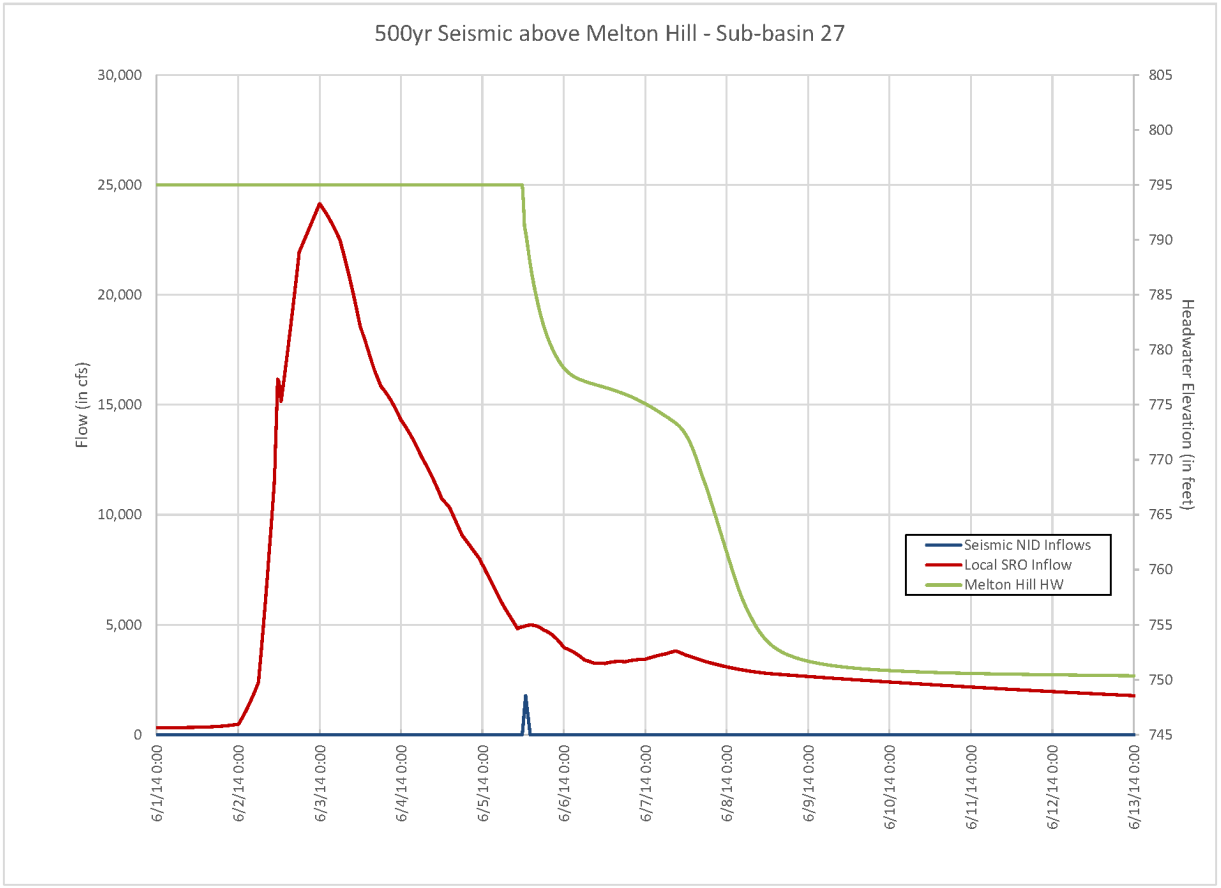

Figure 2.4.4-6. Seismic Inflow Hydrographs for 500-Yr June Flood Event – Melton Hill Dam

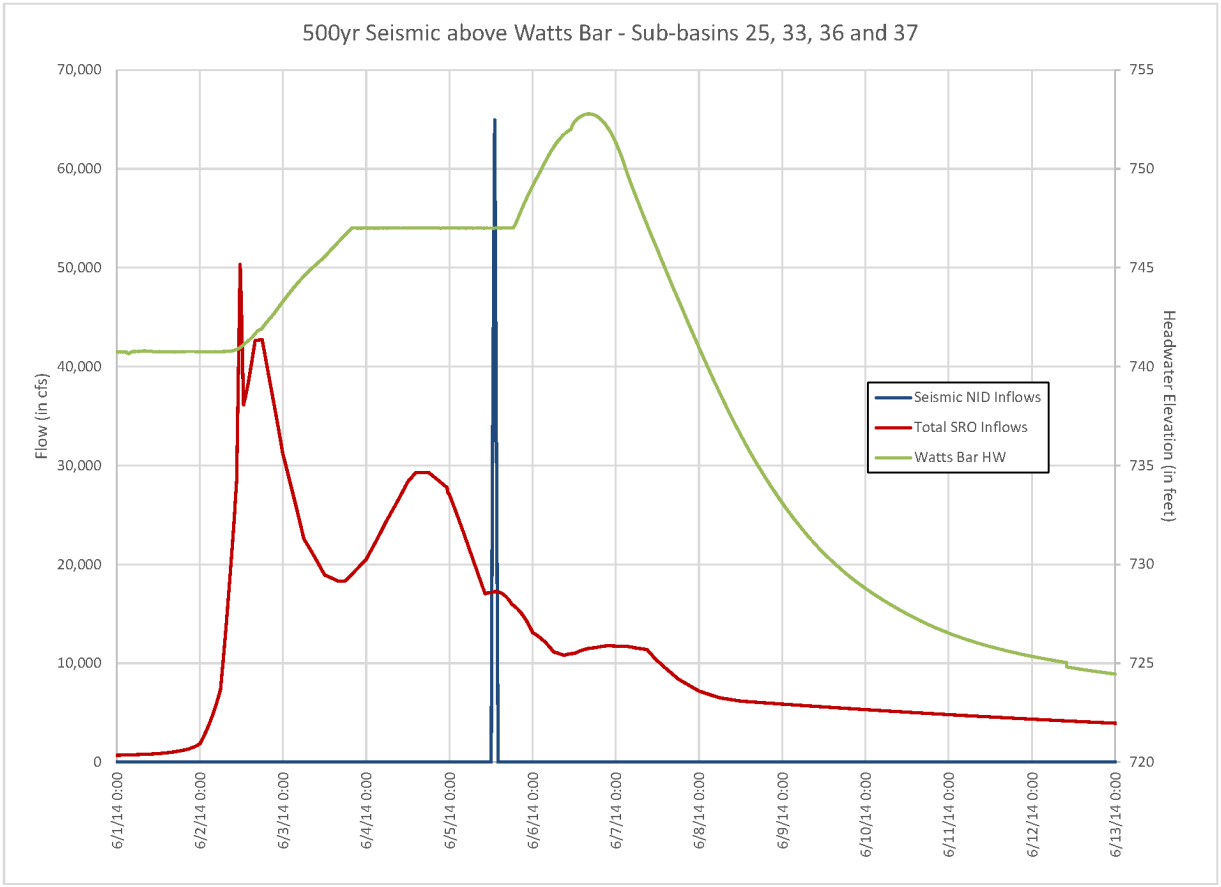

Figure 2.4.4-7. Seismic Inflow Hydrographs for 500-Yr June Flood Event – Watts Bar Dam